Naval Research Laboratory
Washington, DC 20375-5320

EFFICIENT ATOMIZATION AND COMBUSTION OF EMULSIFIED CRUDE OIL

Steven G. Tuttle
John P. Farley

Navy Technology Center for Safety and Survivability
Chemistry Division

James W. Fleming

Nova Research Inc.
Alexandria, VA

This study was funded in part by the U. S. Department of the Interior, Bureau of Safety and Environmental Enforcement (BSEE), through Inter-agency Agreement No. E12PG00050 with the Naval Research Laboratory (NRL), as part of the BSEE Oil Spill Response Research Program.

CONTENTS

FIGURES

TABLES

EFFICIENT ATOMIZATION AND COMBUSTION OF EMULSIFIED CRUDE OIL

INTRODUCTION

This report describes the completed tasks and results of our research effort to demonstrate the effectiveness of the flow-blurring atomizer for burning pure and emulsified crude oil. We demonstrated the feasibility of the flow-blurring atomizer as a method of forming a combustible aerosol of air and crude oil or emulsified crude oil. We demonstrated stable combustion for oil/water flows up to 800 mL/min and with emulsified fractions up to 25% seawater. Emissions from the plume included unburned oil with minimal smoke observed, when compared to pool fire flames.

Droplet measurements with water, crude oil, and emulsified crude oil revealed a Sauter-mean diameter in the range of 20-30 μm, typical of flow blurring atomizers. We observed that large, unburned droplets fell even with large flame plumes, suggesting droplet agglomeration. There was some evidence of secondary droplet fragmentation, caused by flash evaporation of the water, with emulsified crude oil spray, as well as droplet swelling of the pure crude oil droplets, caused by internal evaporation of the lighter-weight hydrocarbons.

We give notional design suggestions for the combustor and igniter. We recommend that the combustor be composed of a cylindrical shell, closed at one end with the spray nozzle and open at the other, where the burning plume exits. Holes along the length will allow the aspiration and entrainment of air into the plume and assist in the flame anchoring and propagation.

In situ burning, where crude oil is burned in large pool fires at sea or on the ice, is the current standard practice for rapid remediation of surface-spilled crude oil in marine environments. It uses much of the same infrastructure as would be needed by the proposed method for capturing and oil removal, in particular the same vessels and booms used to herd the floating crude oil into a thick, floating layer that is pumped and then transported to the shore for processing. Wind and water currents frequently move oil slicks toward ecologically fragile coastal and riparian zones faster than it can be gathered and transported to a facility equipped to receive spilled crude oil. When oil slicks need to be removed more rapidly than they can be transported, *in situ* burning offers a rapid disposal method that minimizes risk to marine life and shore ecosystems.

As an oil-spill remediation method, *in situ* burning has a number of shortfalls. First, as the oil burns, radiance and convection transfers heat to the oil slick to evaporate the oil. The lighter weight hydrocarbons burn first, but once the oil slick is sufficiently thin, the underlying seawater cools the remaining heavier weight hydrocarbons to slow their evaporation and halt the continued combustion of the hydrocarbon vapors. Furthermore, *in situ*, burning produces large amounts of soot (See Fig. 1), carbon monoxide, and unburned hydrocarbons, which are environmental and health hazards that makes it an undesirable method for disposing of slicks near the coastal shores and inland waterways. Finally, this method will not reliably burn emulsified crude oil and seawater [1].

Fig. 1-Soot plumes from *in situ* burning

Surface or subsurface mixing of the crude oil and seawater (or fresh water) emulsifies the oil, which not only makes it more difficult to burn but also increases the pollutant volume. The motion of wind and waves emulsify the surface-spilled crude oil. For sub-surface, or benthic spills, the leak jet mixing and the crude oil buoyancy expands the interface with the surrounding seawater and rapidly mix. Therefore, the greater the depth of the leak, the longer the available mixing time, the greater the emulsification, and the greater the volume of the pollutant plume. Dispersants further enhance the emulsification process. Once emulsified, the crude oil is either difficult or impossible to ignite for *in situ* burning. Oil flares, formed by spraying oil or emulsified oil, are capable of burning mixtures containing up to 80% seawater, produce much less soot and carbon monoxide. Flare burners have been demonstrated by Buist[1], who used a mechanically atomized and swirled burner, and by Expro[2,3], who markets flare burners utilizing an effervescent atomizer. Spray combustion of emulsified oil is further aided by the vaporization of the constituent liquid water that produces a secondary atomization process that increases combustion rates[4].

The difficulty with both of these previous spray methods is that they rely on infrastructure that oil spill vessels do not carry and cannot power. The burner demonstrated by Buist [1] utilized a mechanically complex burner head that, if scaled up to practical sizes, would have significant structural, mechanical, and heat transfer durability issues. The Expro burner [2,3] used on oil platforms utilizes high-pressure oil pumps and air compressors (~1500 psig) to drive the effervescent atomization process; both require larger power sources than would be practical on a small watercraft.

Conventional liquid spray atomization technology has been designed and optimized for low viscosity fluids, such as kerosene, jet fuel, diesel, and water that are pumped at high pressure[5]. In contrast, crude oil is highly viscous[6] and is conventionally pumped at low pressures on marine vessels. Given the advantages of spray combustion for emulsified oil, we should examine alternative atomization approaches and adapt them for both crude oil and the existing infrastructure found on marine vessels used for oil spill remediation.

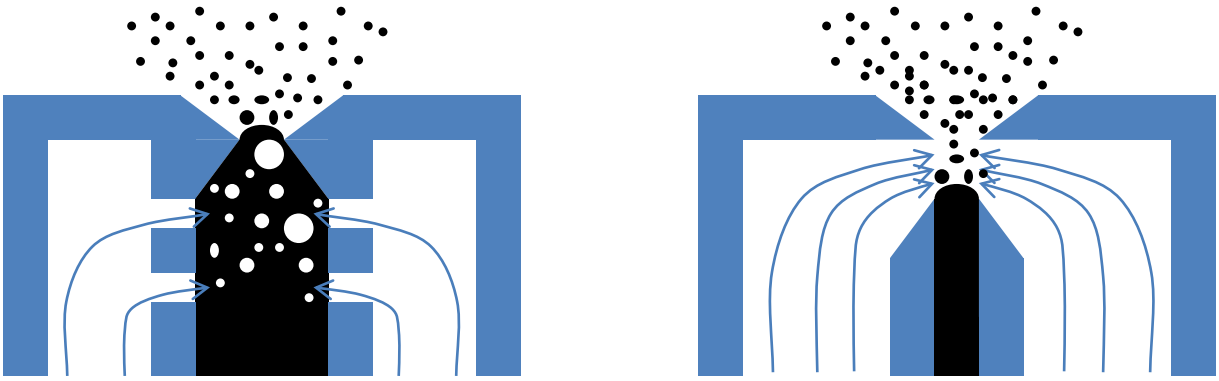

Fig. 2-Effervescent (left) and flow-blurring (right) atomization

Effervescent and flow blurring atomization are two candidates for emulsified crude oil atomization and combustion, shown in Fig. 2, with black representing the liquid and blue arrows representing the atomization gas streamlines. Effervescent atomization, a conventional atomization method already used by Expro, atomizes a liquid by directing air into a confined stream of liquid where it forms bubbles of compressed gas. When the stream of liquid and gas reach the nozzle edit, the air rapidly expands to form and then burst bubbles from the liquid. The bursting bubbles and expanding gas further fracture the liquid into ever-smaller fragments. This simple method is used in a number of applications, including gas turbine spray combustion [5]. Because the volumetric expansion of the entrained air plays such a crucial role in the atomization process, the greater the ratio of the atomizing gas pressure to the ambient pressure, the smaller the atomized droplets. The difficulty is that the liquid pressure must be equal to that of the atomization gas pressure at the bubble-air interface. Therefore, in order to decrease the atomized droplet diameter, both the liquid and air pressure must necessarily increase. The liquid and air nozzle pressures specified by Expro are ~1000 psig. The focus of this study was to explore atomization using much lower pressures (10 psig-100 psig) that would require lower infrastructure footprints.

The primary approach to atomizing crude oil that we examined is flow-blurring atomization. As shown in Fig. 2, this method relies on the formation of a turbulent, high shear stagnation zone at the surface of the liquid. As the liquid flows out of the first orifice, the air cross streams o fragment the liquid surface and then entrain and carry the atomized liquid out of the nozzle [7]. This method has been successfully demonstrated for both conventional liquid and alternative, highly viscous fuels such as vegetable oil and glycerol [8-10]. Instead of relying on high-pressure air, which requires a high-pressure

compressor, flow-blurring atomization relies on high-speed air. Therefore, a low pressure, moderate flow air compressor may be used to effectively atomize the crude oil.

OBJECTIVE

Our objective in this study was to examine the practicality and operability of low-pressure atomization and combustion of emulsified crude oil, with the purpose of augmenting *in situ* burning, especially for emulsified crude oil. The secondary purpose was to assess the necessary air and oil pump infrastructure requirements to achieve efficient spray combustion.

APPROACH

The experimental effort of this investigation required the acquisition of crude oil; the design, fabrication, and assembly of experimental hardware; and the implementation of a range of instrumentation. We will describe in the following subsections the various materials and systems used in this study including the crude oil, burner, flow control, measurements, and droplet measurement systems.

Crude Oil & Emulsions

Chevron supplied Oriente crude oil used in this study. It is a medium, moderate sulfur content crude oil from Ecuador, sampled in 2010. It has an API of 23.4, a specific gravity of 0.9135, and contains 1.48% sulfur. It has a 25.3% vacuum residual with 30% asphaltenes (7.6% of total mass). The assay, provided by Chevron, is listed in the appendix. The oil was shipped in two 55-gallon drums. The drum was agitated before pumping to insure the mixture was uniform.

Medium crude oils have a moderate density compared to the wide range of available crude oils that range from light (low density and free flowing at room temperature) to heavy (higher density and does not readily flow at room temperatures). Light crude has a high proportion of light hydrocarbons while heavy crude has a higher proportion of heavier, wax-like, and tar-like hydrocarbons. Crude oil definitions are relative and used mainly for comparative purposes.

Crude oil/water emulsions were prepared as shown in Table 1 at nominal synthetic seawater fractions of 0, 25, 50, and 75%. Synthetic sea water was mixed to conform to ASTM specifications [11]. We used a paint mixer to mix the oil and seawater for five minutes. In actual spill operations, dispersants and mechanical mixing caused by waves and turbulence continually mixes and emulsifies the crude oil, which allows it to diffuse along the water column. Without the influence of dispersants or biologically produced organic emulsifiers, the crude oil and seawater would not remain mixed. We added a mixture of Span® 85 and Tween® 85 at a 60%-40% relative proportion to emulsify the crude oil and synthetic seawater mixture[4], as shown in Table 1. We observed that the 25% and 50% synthetic seawater mixtures remained emulsified with 1% total emulsifier, while the 75% mixture, even with 2% total emulsifier, separated after two hours.

Table 1-Crude oil and sea water mixtures examined in this study.

	Mixture Designation						
Component	0%	25%		50%		75%	
Oriente Crude Oil	12000 mL	9000 mL	74%	6000 mL	50%	3000 mL	25%
Synthetic Sea Water	-	3000 mL	25%	6000 mL	50%	9000 mL	74%
Span® 85	-	72 mL	0.6%	72 mL	0.6%	144 mL	1.2%
Tween® 85	-	48 mL	0.4%	48 mL	0.4%	96 mL	0.8%

Burner Description

We designed the spray burner components around two interchangeable atomizer designs: the effervescent (EA) and the flow-blurring atomizer (FBA), shown in Fig. 3, top and bottom. Crude oil flowed through the central tube while air flowed through the outer tube. We had planned that the effervescent atomizer would provide a performance baseline since it has been used with jet fuel and crude oil in commercial spray burner applications [3,6], but the pressure drop across the nozzle orifice resulted in an impractically low flow rate that would not compare with the FBA nozzle.

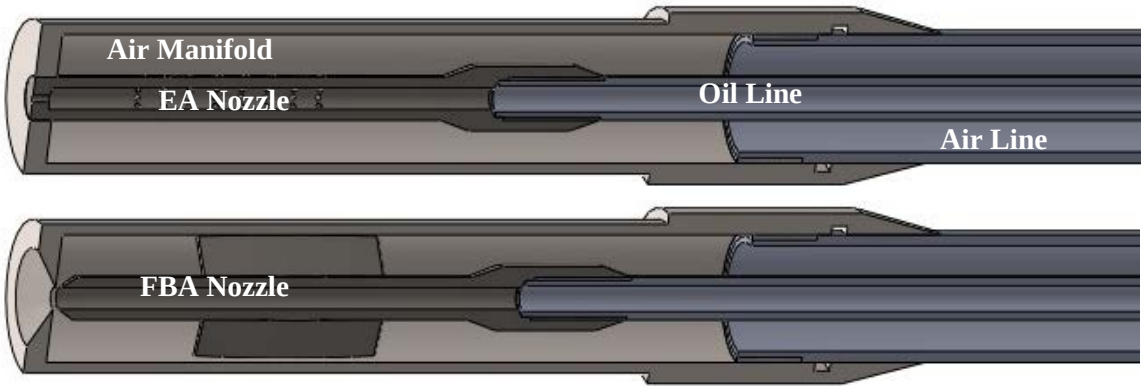

Fig. 3-Cross-sectional views of the two spray atomizers that were to be used in this investigation: effervescent (top) and flow blurring (bottom)

We examined the droplet behavior of water, crude oil, and emulsified crude oil sprays generated by the 3.18-mm diameter orifice. We examined the burning behavior of the 3.18-mm and the 7.04-mm diameter orifices.

Both nozzles have the same auxiliary components: an oil line that directs the crude oil to the atomizer nozzle, an airline that directs the air to the air manifold, from which the atomizing air atomizes the stream of oil. Each diameter of the EA nozzle has a particular manifold, as does each FBA nozzle. The SFBA nozzles use the same air manifolds as the FBA nozzles. The vanes on the FBA nozzles serve to both guides the airflow within the manifold and to hold the nozzle in place. The oil and air hoses are interchangeable between nozzles.

A cross-section view of the burner is shown in Fig. 4 with labeled components. The atomizer (i) was placed in an annular, co-flowing jet (ii) that directed either a straight or swirling stream of air around the periphery of the atomizer. We will describe the igniter jet in detail in the following sub-section.

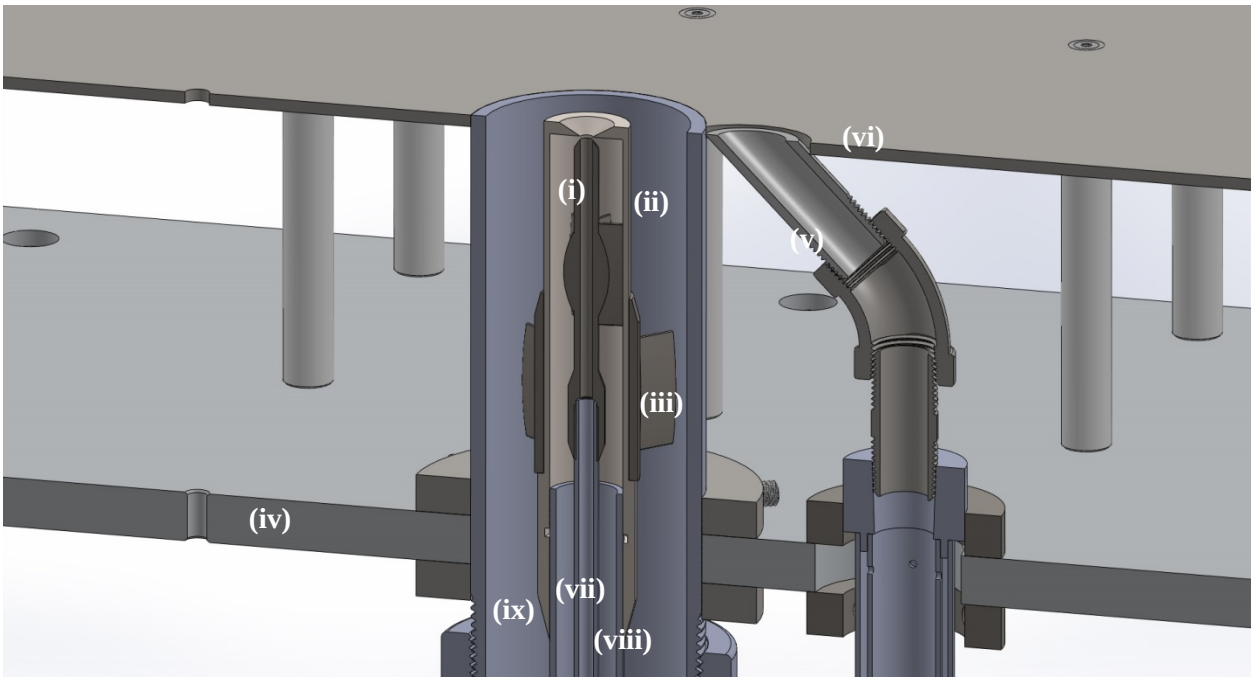

(a)

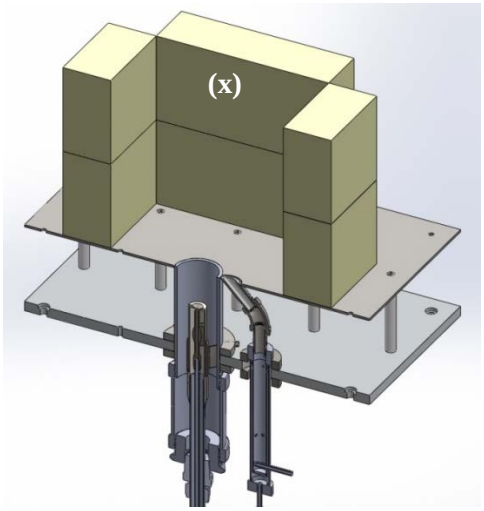

(b)

Fig. 4-Cross-sectional view of the burner assembly (a). The following components are labeled: (i) atomizer, (ii) co-flow jet with guide vanes, (iii) co-flow guide vanes, (iv) baseplate, (v) igniter jet, (vi) faceplate, (vii) fuel tube, (viii) atomizing air tube, and (ix) co-flow channel. (b) In the final studies the lower configuration was used; the burner was surrounded by fire bricks (x) to reflect heat back to the plume.

To ignite the spray, a propane-fueled igniter jet (v) directed a stream of burning propane and air to the base of the spray jet plume. Igniter jets are common ignition sources in large scale combustion experiments[12,13]. The faceplate (vi) acted as a heat shield to protect the supporting baseplate (vii) and mounting platform for instrumentation.

We found that in order to stabilize combustion for emulsified mixtures, we needed to surround the base of the plume with firebricks. The radiant heat from the flames heated the bricks, which in turn reflected the heat back to the droplets.

The overall layout of the test apparatus used for droplet measurements is shown in Fig. 5, with the main components labeled. The traverse (i) allowed us to translate the burner in three dimensions so that a carefully aligned temperature or optical probe could remain stationary. It also allowed us to be able to move the burner remotely to avoid the dangers of exposure to flammable liquids and the heat from the flames. The surrounding optical rails (ii) provided us with stationary locations to mount our flame and droplet imaging optics. The burner support structure (iii) holds the burner assembly (iv) described above. The entire structure is supported on leveling feet so it could be placed and leveled on rough or smooth surfaces. The entire apparatus provided a flexible testbed that we can use in follow-on investigations.

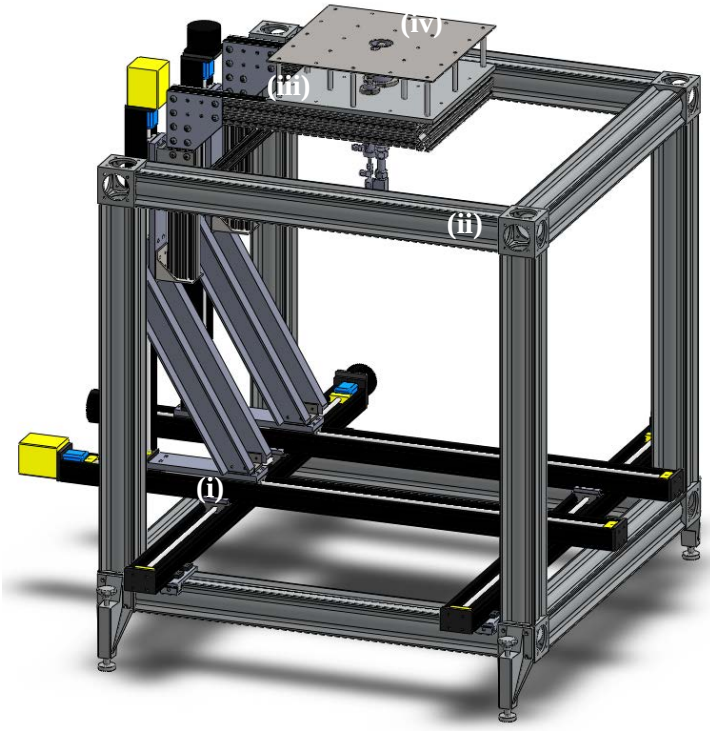

Fig. 5-Layout of the three-dimensional traverse and supporting structure; (i) traverse components, (ii) optical railing for supporting the PDI transmitter and receiver, (iii) burner assembly support structure, and (iv) burner assembly.

Ignition Torch

We designed an ignition torch similar to one used by NASA to ignite unburned fuel in a test rocket plume [12] and to one used to ignite other combustion experiments [14]. It is composed of a small, cylindrical combustor with staged air injection, a simple fuel jet, and a spark igniter to light the fuel and air. NASA technicians used this design with hydrogen fuel; we fueled it with propane.

The original ignition torch is shown in Fig. 6a. A secondary fuel injection port was added, as shown in Fig. 6b, to inject a secondary stream of propane. The air injection tube (i) directed air around the tube combustor (ii) and through primary (iii) and secondary (iv) injection holes. The spark plug (v) was placed just downstream of the pilot fuel injector (vi) where sparks ignited the fuel-air mixture. We added a secondary fuel injection port (vii) to produce a hotter gas stream and improve flame anchoring of the spray plume.

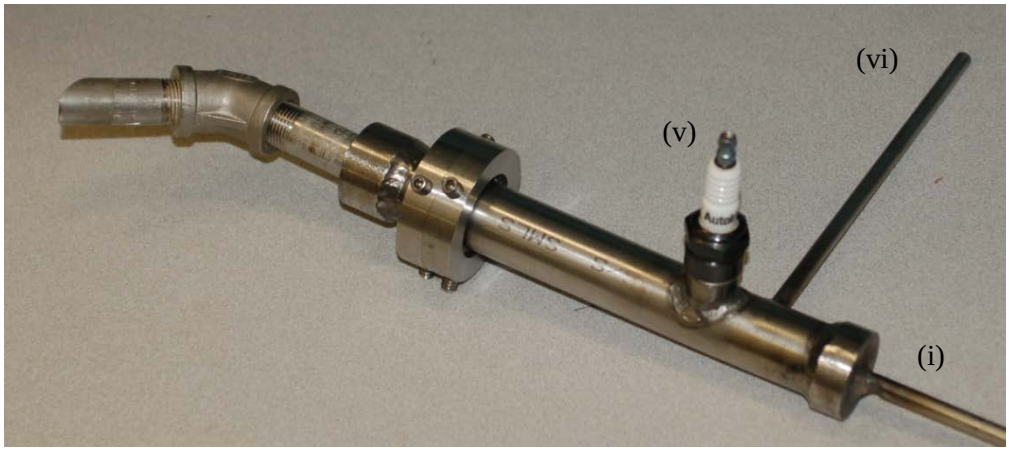

(a)

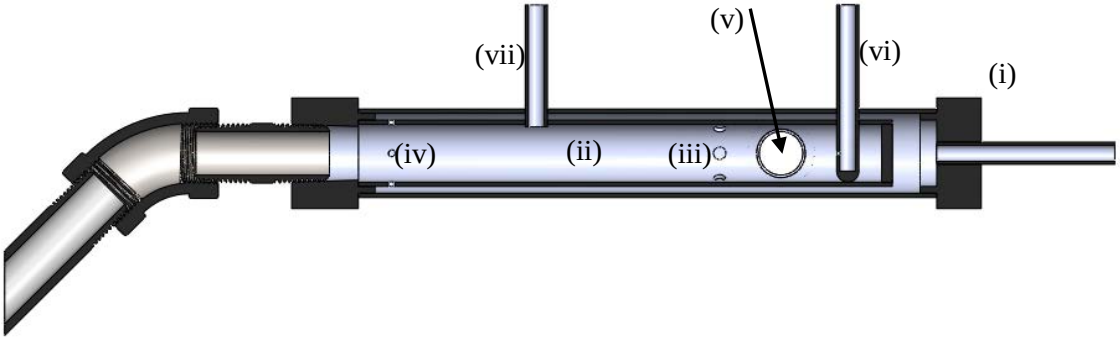

(b)

Fig. 6-Photograph (a) and cross-sectional view (b) of the ignition torch used to ignite and pilot the spray plume

Table 2-Ignition torch operation parameters.

Stage	U	ϕ	V_{fuel}	V_{air}
Torch Ignition	40 m/s	1.39	1.12 L/min	19.2 L/min
Plume Pilot	59 m/s	0.96	1.12 L/min	27.8 L/min

The torch combustor was ignited at an equivalence ratio (ϕ) of 1.39 and then the airflow was increased to lower the equivalence ratio and raise the jet velocity, as shown in Table 2. During the initial ignition stage, a flame was not visible. Once the airflow was increased, a jet of luminous, burning gases was observed.

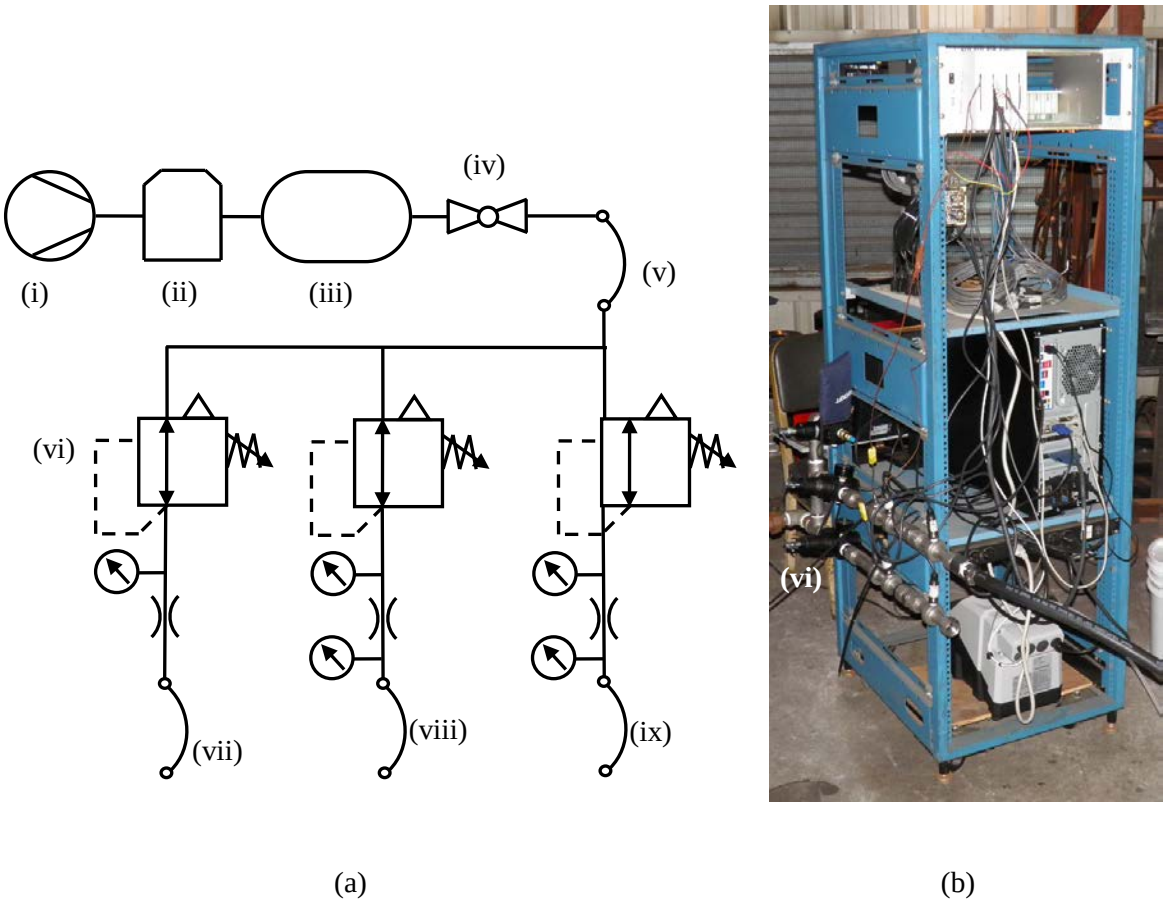

(a) (b)

Fig. 7-Schematic (a) of the airflow control system and photograph of the rack–mounted data acquisition system. The venturis and regulators are mounted on the side and the peristaltic pump is at the bottom of the rack

Air and Oil Flow Systems

We designed and assembled both the air and oil-emulsion flow systems with commercial, off-the-shelf components. This approach cost less and met the overall objective of building a practical-scale system from conventional components. A data acquisition system (National Instruments Inc.) recorded and processed the total pressure and temperature upstream of the venturis and the total pressure downstream of the venturis, as detected by the pressure transducers and the thermocouples. The same system controlled the flow rate of the crude oil as pumped by the peristaltic pump.

Air Delivery System

The air delivery system is composed of a commercial compressor system, hoses to deliver the air, pressure regulators, and orifices to meter the flow. Fig. 7 shows the schematic of the airflow system and a photograph of the instrumentation rack, with Roman numerals designating different components. Air passed through the compressor (i) and then through the dryer (ii) to remove most of the ambient humidity

before entering the tank (iii). A ball valve (iv) allowed or restricted the air from entering a hose (v) which directed the air to a manifold, which in turn split the flow into three branches. A manual regulator (vi) on each branch reduced and regulated the air pressure before the air passed through an orifice. The first branch (vii) has a conventional pressure gauge and orifice (O'Keefe Controls, KH-##-BR) to meter air flow to the ignition torch. The second and third branches (viii and ix) utilize NIST-traceable pressure transducers (Omega Engineering, PX309-100A5V and PX309-200A5V) upstream and downstream from a NIST-traceable, critical-flow venturi (Flow Systems, SN-16-AN-0.022-SS) and metering tube (Flow Systems, FC, IS, ES-16-0.87-SS) to meter flow to the spray atomizer and the annular co-flow. Hoses then direct the flows of all three branches to their respective components.

Oil Delivery System

A peristaltic pump and hose delivered the emulsified crude oil to the spray nozzle. The peristaltic pump (Cole-Parmer EW-74203-02) is capable of pumping fluids with viscosities as great as 12,000 cP with pressures as high as 125 psig in ranges between 0.4 mL/min to 1097 mL/min, allowing a wide range of flow rates. The test plan called for oil or emulsion flow rates in the range of 100 mL/min to 800 mL/min, depending on the nozzle size.

Droplet Measurement

We used Phase Doppler Interferometry (PDI) to measure droplet diameters and velocities [15]. The optical layout is shown in Fig. 8 and was composed of a laser transmitter (iii) that focused two 632.8-nm lasers beams to an intersecting region forming the measurement volume, where the droplets passed through and refracted light to the receiver (v). The PDI system (Dantec Dynamics Fiber PDA) utilized was composed of a transmitter (iii) (65X60 FlowLite) that directed two 632.8-nm beams (iv) across the measurement volume. The refracted signal was gathered by receiver optics and detector (v) (57X40 FiberPDA and 58N70 FiberPDA) where the signals were amplified by photomultipliers and directed into the processor (58N80 MultiPDA). The processed signals were then directed to a PC through an interface board (58G130 PDA). Both the transmitter and receiver were fitted with adapters (60X117) and lenses (50X58) for 500-mm focal lengths from the measurement volume.

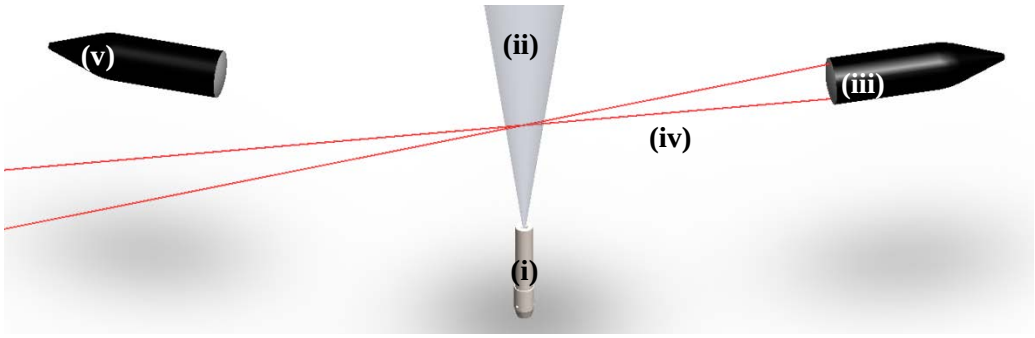

Fig. 8-Diagram of the phase Doppler interferometer with the spray nozzle (i), plume (ii), laser transmitter (iii), laser beams (iv), and receiver (v)

Phase Doppler interferometry operates using light scattered by a spherical droplet as it passes through a measurement volume formed by crossing of two laser beams. The laser beam is first split into two equally powered beams; one beam passes through a Bragg cell oscillating at 40 MHz, which modulates the wavelength for that beam before interacting with the other beam to form the measurement

volume. As a result, the interference pattern formed where the beams cross translates in space at a constant rate. When a droplet or bubble passes through the measurement volume, it refracts the light, which is gathered by the receiver and amplified by a photomultiplier. The signal processor uses the frequency shift in the scattered signal to calculate the velocity. The signal processor uses the phase differences between three spatially separate detectors in the receiver to calculate and validate droplet diameters.

RESULTS

Three distinct experimental phases were conducted in this effort. During the first phase, we assembled the spray nozzle on the traverse, flow system, and droplet measurement system to measure water droplets. In the following phase, we placed the burner on blocks for outdoor burning and tested the burning operability with crude oil and emulsified crude oil. During the final phase, we placed the burner on the traverse and measured the droplet distribution during combustion. In the process of the second and third phases, we made design and operation changes to improve the performance of the burner. In the following sections, we describe each process.

Water Spray Droplet Measurement

We completed water droplet measurements with the 3.18-mm nozzle to verify the operability of the flow and droplet measurement systems and the capability of the droplet capture system. A 10-in. diameter plastic pipe attached to a high capacity ventilation vacuum and a settling catch composed the droplet capture system. This was able to capture most of the water droplets and mist, with only a small amount of residual mist blow out.

For droplet diameter notation, we used the Sauter-mean diameter (D_{32} or SMD), which is used in literature when calculating mass transfer and reaction rates of sprayed fuel [16]. The statistical expression is as follows:

$$D_{32} = \frac{\sum N_i D_i^3}{\sum N_i D_i^2} \quad (1)$$

Where N is the number of droplets in a particular statistical bin of the probability distribution and D is the diameter for that bin. The Sauter mean diameter is statistically representative of the volume-to-surface area ratio of the droplet distribution of the spray. The volume-to-surface ratio of a droplet is representative of the ratio of the thermal capacitance ($c_p \rho \pi d^3/6$) to the rate of heat and mass transfer at the surface ($\dot{q}_{m,e} \pi d^2$). Where the dominant parameters are c_p (heat capacity), ρ (density), d (diameter), and $\dot{q}_{m,e}$ (mass flux from the droplet or heat flux to the droplet driven by temperature gradient, concentration gradient, or surface combustion).

The Sauter mean droplet diameter profiles shown in Fig. 9 were measured for the 3.18-mm diameter nozzle, with liquid flow rates of 92.1 and 271.2 mL/min, with air-liquid ratios (ALR) of 0.5 and 1.0. The Sauter-mean diameter is the area-weighted mean diameter and is the standard notation in physical systems where droplet evaporation is the physical process of concern[16]. We can observe that generally, higher liquid flow rates and ALR produced smaller droplets across the entire profile. We can expect this trend since both parameters increase the local shear at the air-liquid interface. Table 3 shows the corresponding pressures and mass flows. The units for the pressure are in both Pascal and psig for clarity.

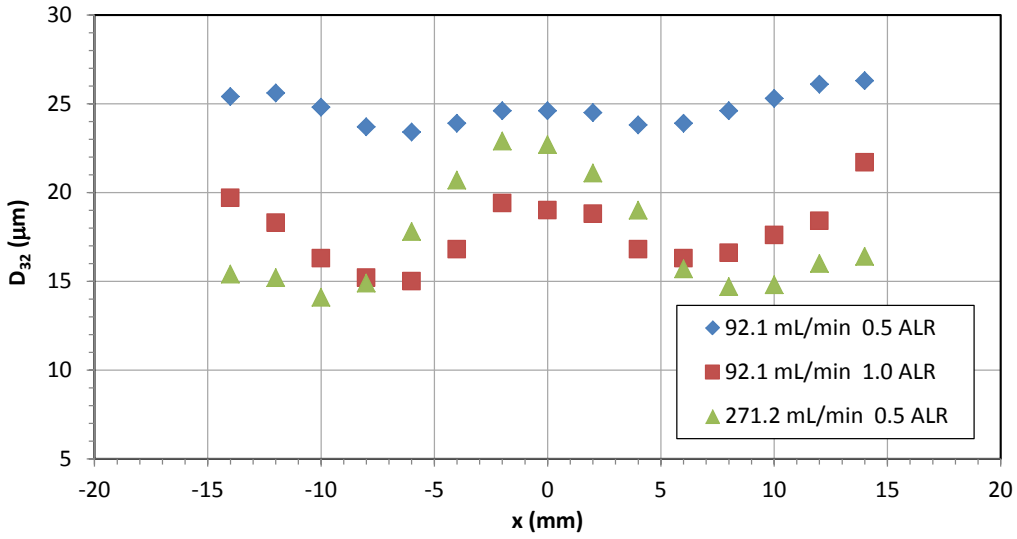

Fig. 9-Sauter-mean diameter measurements for the 3.18-mm (0.125-in) flow blurring atomizer

Table 3-Operating parameters for the water testing.

Nozzle Dia. (mm)	Water Flow (mL/min)	ALR (1000 kg/m^3)	Venturi Pressure	
			Upstream (Pa) (psig)	Downstream (Pa) (psig)
3.18	91.5	0.5	3.32E5	1.19E5
			48.1	17.3
3.18	91.5	1	6.70E5	1.65E5
			97.1	24.0
3.18	270	0.5	9.59E5	2.20E5
			139.1	31.9

Outdoor Burn Testing

We performed burn testing at the burn facility of the Naval Research Laboratory's Chesapeake Bay Detachment. We placed the burner on cinder blocks, in a 28-ft^2 burn pan (See Fig. 10) used for pool fire testing. The burn pan acted as a catch basin for crude oil and a stable, heat resistant platform. We placed the pan in the center of a 40 ft x 40 ft tarp to capture additional overspray. The instrumentation rack and all of the aforementioned equipment were located on a concrete testing platform used for outdoor fire and burn testing.

Initial burn tests were unsuccessful due to the low temperature of the igniter jet. In order to increase the exhaust temperature, a secondary fuel port was drilled, welded, and plumbed. The secondary fuel mixed with the secondary air stream and the hot combustion products and then ignited. This modified jet produced higher exhaust temperatures to produce more stable spray plume combustion.

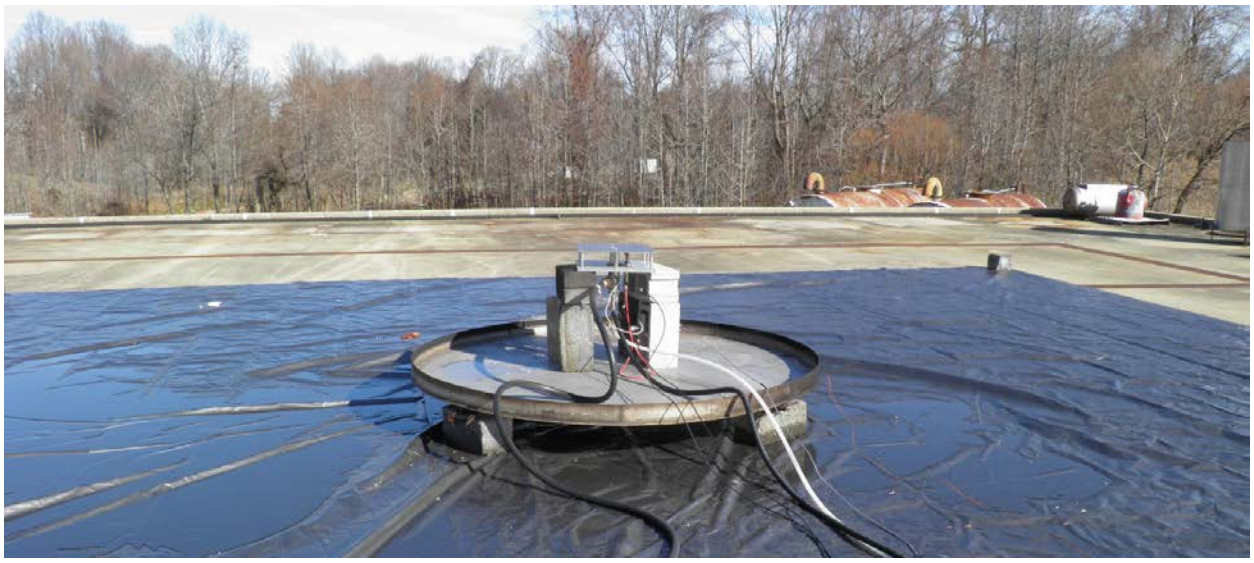

Fig. 10-Burner mounted on pool fire burn pan and tarp to catch un-burned oil droplets

We made further *ad hoc* modifications during the second burn test to produce combustion, shown in Fig. 11. We placed cinder blocks around the spray nozzle to block the wind. Even with these changes, there were problems with unburned droplets being ejected and then carried by the wind, as well as smoke and flame stability issues. As seen in Table 4, most tests had large droplets that were not burned that landed back on the tarp. Only at an air-loading ratio (ALR) of unity were the droplets fine enough to not land back on the tarp, but combustion was unstable and incomplete.

There were a number of problems with the second set up. First, the cinder blocks shielded the wind, but did not reflect heat. The igniter jet needed to be tuned to produce even higher temperatures. Finally, the spray plume had such high speeds that the igniter jet did not have the momentum to penetrate into and mix with the jet to evaporate crude oil and initiate combustion.

(a) (b) (c)

Fig. 11-Photographs of initial burn tests, with the burner shielded by cinder blocks

Table 4-Test conditions and results for the second burn test

Nozzle Dia. (mm)	Crude Oil (mL/min)	ALR (865 kg/m^3)	Comment
3.18	98.7	0.25	Burned, many large, unburned droplets
3.18	98.7	0.5	Same
3.18	199	0.24	Same
3.18	98	1.00	Fine mist, unstable combustion

We made further modifications to the burner to resolve the aforementioned issues. We replaced the cinder blocks with fire bricks (See Fig. 4 and Fig. 12), which reflect heat more effectively. We lowered the spray nozzle by 45 mm to allow the plume to broaden before intersecting with the igniter jet exhaust. Finally, we optimized the igniter jet to eject gases at ~1200 K to anchor the spray plume combustion, to the torch ignition condition listed in Table 2.

Fig. 12-Burner surrounded by fire bricks during unsteady combustion

Fig. 13-Burner mounted on pool fire catch basin and tarp to catch un-burned oil droplets: nozzle diameter = 7.04 mm, oil flow rate = 800 mL/min, and ALR = 0.5

We repeated the test conditions in Table 4 with the burner modifications and observed much better performance. As described in Table 5, the flame plume was stable and produced some visible smoke, but once the firebricks heated up, they reflected heat back into the spray to aid both droplet evaporation and flame stability, producing plume combustion as shown in Fig. 13. As a result, there was little visible smoke at steady state. This condition persisted with increasing oil flow rates, until at an ALR of 0.125, where the anchor region was too rich to sustain a steady flame. We also observed a lean transition at an ALR of 1.5, such that the relatively more lean fuel loading produced unsteady combustion.

In this configuration, we were not successful in burning the 50% or the 75% emulsified mixtures. The ignition torch was able to produce combustion at the base of the plume, but the resulting flame did not release enough heat to evaporate the downstream plume and allow combustion to propagate along the rest of the spray plume.

Table 5-Test conditions and results for the third outdoor burn test

Nozzle Dia. (mm)	Crude Oil (mL/min)	ALR (865 kg/m3)	Venturi Pressure		Comment, description
			Upstream (Pa) (psig)	Downstream (Pa) (psig)	
3.18	98.3	0.53	3.28E5 47.5	1.16E5 16.8	Smokey during heat up, very steady. Clean burning at the end.
3.18	47.5	1.05	3.12E5 45.2	1.14E5 16.6	Same
3.18	98.3	1.00	6.14E5 89.1	1.48E5 21.5	Same
3.18	98.1	0.99	6.06E5 87.9	1.46E5 21.2	Same
3.18	98.1	1.51	9.32E5 135.1	2.00E5 29.0	Same, but less steady
3.18	199	0.25	3.10E5 44.9	1.15E5 16.6	Same
3.18	47.5	1.43	4.23E5 61.4	1.26E5 18.3	Same
3.18	199	0.50	6.26E5 90.8	1.52E5 22.1	Same
3.18	400	0.25	6.27E5 90.9	1.53E5 22.1	Same
3.18	800	0.125	6.27E5 90.9	1.53E5 22.1	Too rich, unstable
7.04	199	1.01	3.16E5 45.9	1.12E5 16.3	Smokey during heat up, very steady. Clean burning at the end.
7.04	400	0.50	3.16E5 45.9	1.12E5 16.3	Same
7.04	399	0.51	3.16E5 45.9	1.12E5 16.3	Same
7.04	800	0.25	3.16E5 45.8	1.12E5 16.2	Same
7.04	199	1.01	3.16E5 45.9	1.12E5 16.3	Same
7.04	50.0	4.03	3.16E5 45.8	1.12E5 16.3	Same
7.04	100	2.01	3.16E5 45.8	1.12E5 16.3	Same
7.04	198	1.02	3.16E5 45.8	1.12E5 16.3	Same

Indoor Burn Testing and Spray Measurements

Prior to gathering spray droplet measurements in the burning plume, we refined the igniter jet operation and increased the airflow, once the torch combustor was lit, to produce a luminous exit flame that was more effective at stabilizing the plume, as shown in Fig. 13. This increased the temperature nearer to the adiabatic flame temperature (~2200 K). We also lowered the spray nozzle to 50 mm below the burner exit (see Fig. 4). Table 6 lists the test conditions.

Fig. 13-Ignition torch, tuned to eject luminous reacting flame

Table 6-Test conditions for droplet measurements within the burning plume

Nozzle Dia. (mm)	Crude Oil (mL/min)	ALR (865 kg/m^3)	m_{Air} (kg/s)	Venturi Pressure		Pump Power	
				Upstream (Pa) (psig)	Downsteam (Pa) (psig)	P_{oil} (W) (hp)	$P_{oil+air}$ (W) (hp)
3.18	500.0	0.20	1.422E-3	6.31E+5	1.65E+5	26	713
				91.5	23.9	0.034	0.96
3.18	494.4	0.21	1.420E-3	6.26E+5	1.53E+5	23	637
				90.8	22.3	0.032	0.85

We should note that the nozzle air pressure is no more than 23.9 psig, which is a much lower air pressures than used in industrial oil flares. If we assume that there is little flow loss with the air, then the pressure drop across the nozzle is the same for both the air and crude oil. If we combine expressions for the power ($P = \vec{F} \cdot \vec{v}$) and Bernoulli's momentum and energy equation ($p_t = p_s + \frac{1}{2}\rho v^2$), we develop an expression for ideal pump power, considering the air and oil flows:

$$P = \Delta p \left(\frac{\pi}{4} d_n^2\right) A_n \left(\sqrt{\frac{2\Delta p}{\rho_{oil}}} + \sqrt{\frac{2\Delta p}{\rho_{air}}}\right) \quad (2)$$

Where Δp is the nozzle pressure drop, d_n is the nozzle diameter, and ρ is the density of the fluid. While this expression does not account for pressure losses in the oil or air hoses, it does provide an order of magnitude value that scales with nozzle diameter, fluid densities, and pressure drop. We should note

that the power requirement is inversely proportional to the square root of the density, which is why most of the necessary power pumps the air.

While testing with crude oil, we observed that the spray plume initially stabilized above the burner platform, but as the burner hardware warmed up, the combustion shifted upstream to stabilize within the co-flow channel of the burner, within which we placed the spray nozzle. We could see that the static pressure depression produced by the spray plume drew smoke and hot gases above the burner faceplate into the cavity between the plume jet and the co-flow channel wall. We also observed that errant droplets were impinging onto the channel wall and burning with the air. The resulting hot combustion products then stabilized the spray plume combustion, such that the air and fuel to the igniter jet could be turned off and the plume continued to burn, as shown in Fig. 13. In this configuration, the fire bricks were not required to keep the plume burning and could be removed.

The lower nozzle position and hotter ignition jet allowed stable combustion for 25% emulsified crude oil, but with some critical caveats. First, the flame did not anchor inside of the co-flow channel, nor were there flames on the channel wall. The plume stabilized using a similar recirculation mechanism, but by using the heat transfer of the firebricks to assist in evaporation. Therefore, the flame was actually lifted, as shown in Fig. 14b and Fig. 14c.

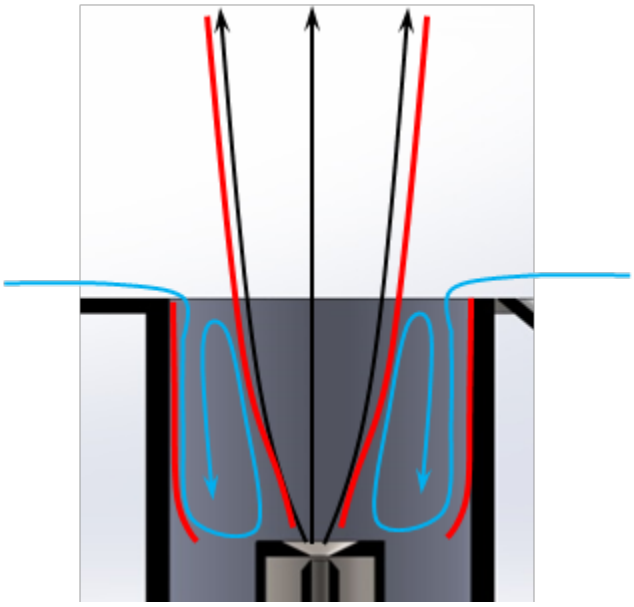

Fig. 13-Stabilization mechanism of the modified burner and spray plume

The flame stabilization or anchoring process of the emulsified crude oil is similar to that of the crude oil, but there are some crucial differences. First, the evaporation and expansion of the water at the base of the burning plume broadens the base of the spray plume. Second, water evaporation reduces the local oxygen concentration, which slows the vapor ignition process and produces the observed, lifted flame.

(a)	(b)	(c)

Fig. 14- The burning plume for crude oil (a) and 25% emulsified crude oil (b and c). The base of the emulsified flame jet is shown in (c) to reveal the lifted flame. 3.18 mm spray nozzle, ALR = 0.2, 500 mL/min.

Droplet measurements were made with the same diagnostic set up as used with the water droplets, except that the refraction was gathered at 15˚ instead of at 30˚. These measurements were complicated by the falling of hot, unburned droplets onto the receiver and the high radiative heat load on the traverse and railing structures. Plastic sheeting was used to cover the receiver and the structure supporting it, but the heat caused the plastic sheeting to degrade and melt over time. The heat also caused the optical alignment to drift as the structure expanded and contracted with changes in temperature. Though the unburned droplets were not desirable, there was little visible smoke in the burned plume.

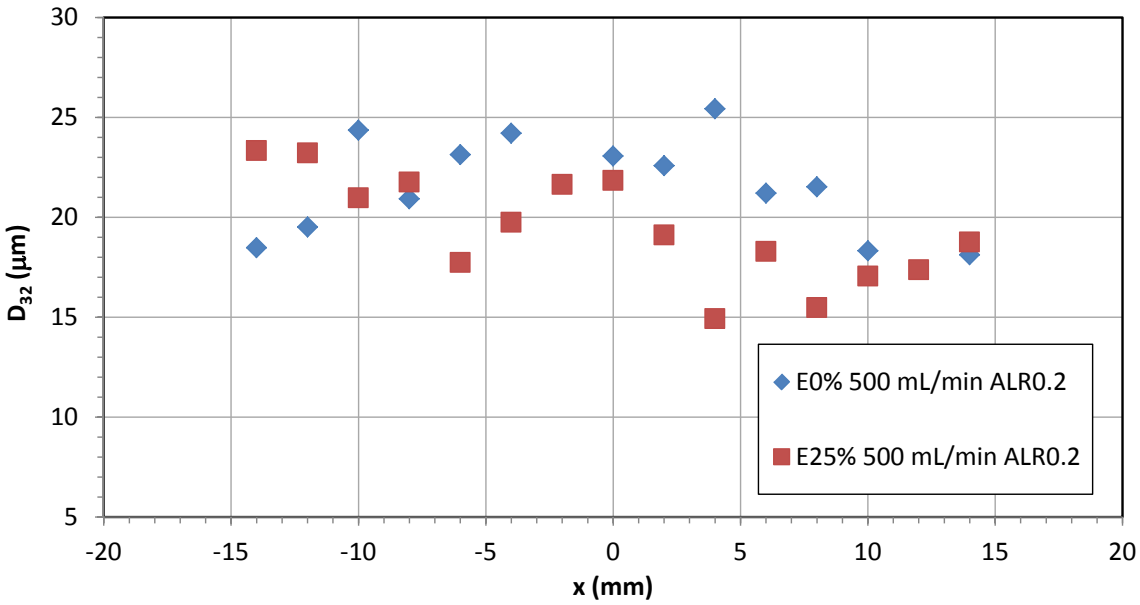

Fig. 15-Droplet diameter profiles gathered at 25 mm above the burner exit, 75 mm above the nozzle exit

We made droplet measurements at two profiles across the spray plume and along the centerline to compare the droplet behavior between crude oil and the 25% -emulsified crude oil. The profiles gathered 25 mm above the burner exit, shown in Fig. 15, reveal only a slight difference in droplet diameters with emulsification, with no clear consistent difference. The skew of the diameters to smaller sizes to the right of the center are due to slight misalignment of the atomizer components and the influence of the igniter jet flow momentum, which pushed the spray plume to one side.

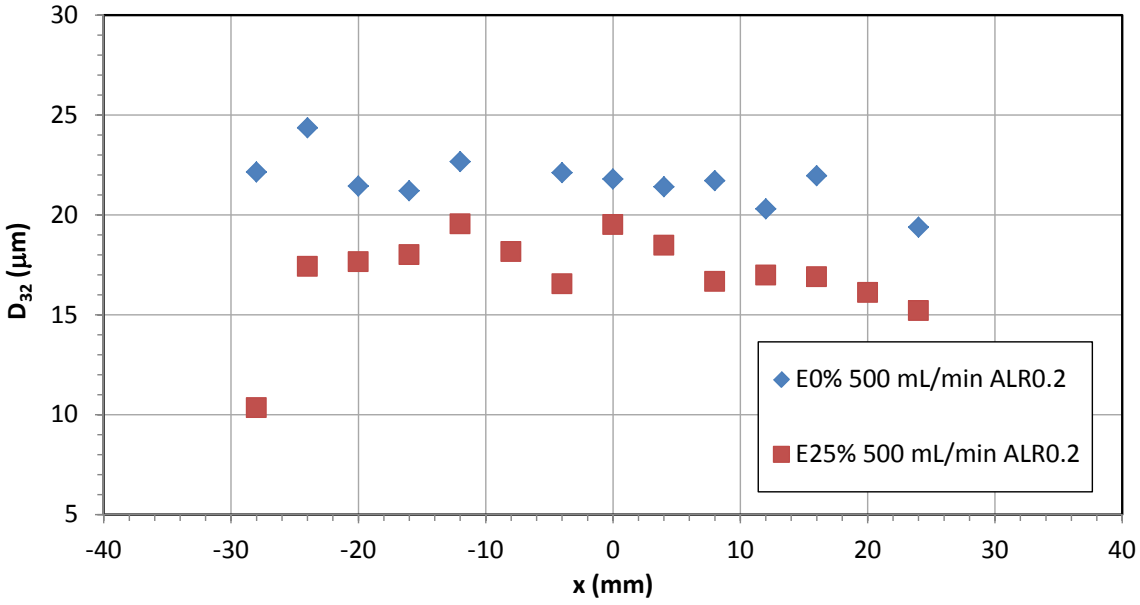

Fig. 16-Droplet diameter profiles gathered at 75 mm above the burner exit, 125 mm above the nozzle exit

Further downstream, the profile at 75 mm from the burner exit, shown in Fig. 16 shows consistently smaller droplet diameters, with a sharp decrease in the diameter at the edge of the plume. The lower boiling point of the water would result in more rapid droplet diameter reduction or, with sufficient heat transfer, result in flash evaporation of the water and secondary droplet atomization, as was observed by Ocampo-Barrera *et al.* [4] with heavy fuel oil and water emulsions. It is interesting to note that the droplet diameters of the pure crude oil remain in the same range. We should not conclude that the crude oil droplets are not evaporating. Droplet measurements from other spray studies have indicated that the hydrocarbon droplets actually swell in the process of evaporation as internal vapor bubbles form [17].

Droplet profiles along the center axis of the plume reflect similar behavior, as shown in Fig. 17. It is curious to note a general increase in the droplet diameter with streamwise distance along the plume. There are two possible explanations for this observation. The first is that the evaporation of the smaller droplets, which evaporate more rapidly than the larger droplets, is skewing the distribution toward a larger diameter. The second possible explanation is that droplets are colliding and agglomerating to form larger droplets. Considering the unburned droplets that were falling down during the experiment, either process may have occurred.

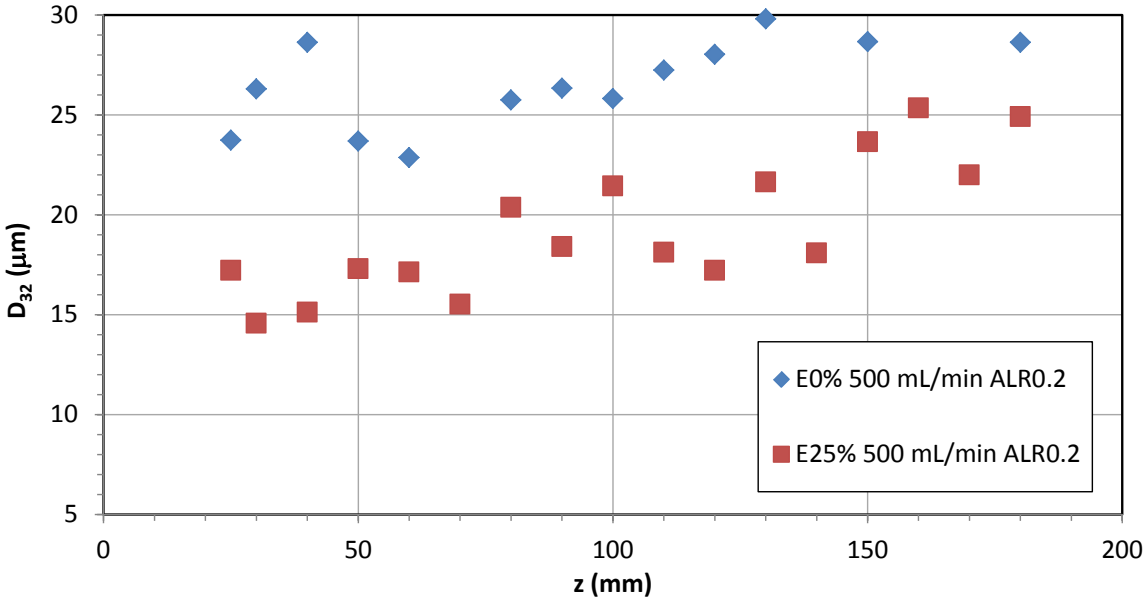

Fig. 17-Droplet diameter profiles gathered along the centerline, measured from the burner exit

CONCLUSIONS

We have successfully demonstrated the flow-blurring atomizer as a practical candidate for producing a flammable aerosol of crude oil and emulsified crude oil. We were able to determine successful flame stabilization strategies that required no additional air or fuel flows, other than the ignition torch for the emulsified crude oil. We also showed that the atomizer required low liquid and air pressures, thus low pump power requirements, to produce a stable, flammable spray plume. Droplet measurements with both water and crude oil revealed little diameter dependence on the viscosity and greater dependence on the mass ratio of the atomization air flow to the liquid flow rates. We also were able to observe successful

atomization whether the crude oil was at room or at near freezing temperatures. These results prompt a number of considerations.

First, the application of this nozzle for highly viscous crude oil is a novel use and demonstrates that it is a functional, flexible nozzle technology for general crude oil combustion. Using mid-weight crude oil, the nozzle was able to produce spray combustion at low temperature, where the crude oil was more viscous, and at nominal, room temperature, where the crude oil was less viscous. The design of the nozzle, with relatively straight flow paths and large channels and orifice, also make it a robust alternative when the oil contains organic and inorganic solids. This is especially important when un-filtered oil has been spilled near a well head or has mixed with ocean debris.

The successful demonstration of successful atomization and combustion with low atomization pressures (~20 psig) also promises a much smaller infrastructure footprint when integrated into a complete system. Preliminary, one-dimensional calculations showed pump and compressor power requirements scaled with the nozzle pressure drop ($\Delta p^{3/2}$). This is especially significant when compared to current market alternatives that require much higher atomization pressures (~1500 psig), and thus much higher power requirements for the air compressor and oil pump. For an oil platform, this difference would reduce power requirements. If we intend to use this nozzle as part of a burner system on a repurposed fishing vessel, the much smaller power and weight limits could only use a low-pressure, FBA-based system. Therefore, the FBA nozzle is a low-pressure, low-power alternative that we can deploy onto existing vessels, modified for crude oil remediation response.

We were also able to observe the flame anchoring mechanism of stable combustion. The annular recirculation zones at the base of the plume, formed between the spray plume and the co-flow channel and again between the plume and the firebricks, allowed hot products to recirculate back to evaporate the spray while entraining air for anchoring combustion. This same mechanism will provide a reliable anchoring process in future design refinements. This behavior was able stabilize combustion for crude oil, without the aid of a propane torch, and with modification, may be able to stabilize combustion for some emulsified crude oil mixtures. The flame anchoring behavior we demonstrated has the further advantage of not requiring a large secondary airflow to complete combustion. Instead, the burning plume entrained the surrounding air.

Droplet measurements revealed a number of important behaviors relevant to this and future studies. First, droplet diameters did not change appreciably whether the liquid was water or crude oil, even though the viscosity is close to four orders of magnitude different. Such robust atomization behavior demonstrates that the FBA will operate successfully in a wide range of conditions and with a wide range of crude oils, which have a wide viscosity variation as well.

We have also observed evidence of droplet agglomeration for both crude oil and emulsified crude oil. The increase in the centerline droplet diameters suggest the droplet collisions increased the droplet diameters, which decreased the relative drag of the droplets while gravity remained constant. Eventually, the droplet diameters increased sufficiently that gravity accelerated them downward. We also observed evidence of secondary atomization, particularly at the edge of the plume, probably caused by rapid water evaporation and then the subsequent fragmentation of the emulsified oil droplets. Secondary atomization assists in the combustion process by forming smaller droplets that evaporate and burn more quickly.

FUTURE WORK

In future studies, there are a number of engineering and scientific issues that will need to resolved to optimize performance and operability. First, the combustion efficiency of the process needs to be quantified, as well as the species and concentrations in the gaseous emissions. Additionally, a more

consistent and fieldable flame ignition process needs to be incorporated that eliminates the use of propane. Though appropriate for laboratory or land-based burning, on an actual watercraft, propane would require an outdoor tank and NFPA 58-certified plumbing, regulators, and controls [18]. The crew would need to return to port to refill/exchange propane tanks. A strong potential candidate would be a constant-flow plasma torch that would evaporate and ionize the emulsified crude oil, as well as provide ample heat at very high temperatures (~3000 K) to initiate combustion, but would only require a stream of air and a source of electricity.

An additional limitation is the agglomeration of the oil droplets along the plume length, their incomplete evaporation and combustion, and their subsequent cascading downward. A common strategy used in gas turbine engine design is to increase turbulence at the base of the plume and along the plume length by imposing swirl to both shorten and mix more air into the plume, increasing both heat release and decrease the amount of ejected, unburned oil [5]. Reducing the radiant heat loss by encasing more of the plume length would also reflect radiate heat back to the plume to increase spray evaporation rates.

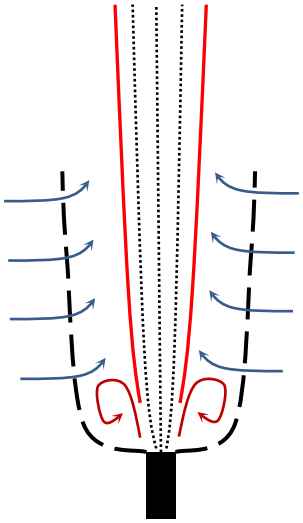

Fig. 18-Notional design of the combustor

From examining the flame anchoring and propagating processes, we can describe the basic geometry of a full-scale burner, shown in Fig. 18. A broad, sudden expansion around the swirling nozzle exit will provide a region for the formation of a recirculation zone where the flame anchors and then propagates along the length of the plume. A shroud, enclosing part of the plume, would provide additional volume for recirculation, if there were sufficient radial distance between the plume and the shroud wall to provide for recirculation at the plume base and mixing along the plume length. Holes along the length of the shroud would allow plume to pull in additional air along the plume length. The shroud must also be sufficiently long such that either pure or emulsified crude oil will burn without flame anchoring instability. The shroud also provides a surface on which laterally sprayed droplets impinge and then burn to provide hot products to assist in anchoring combustion. The shroud would also reflect the heat back to the plume and shield the flame-anchoring region from wind.

Though the notional design addresses the operability issues, the design solutions present a number of engineering issues. First, given the jet diameter (D_j), we need to determine the optimum shroud diameter (D_s), ratio of azimuthal to axial momentum of the swirl (referred to as the swirl ratio, S), and what is the

distribution of the holes along the shroud that would provide sufficient aeration of the plume without quenching combustion.

We also need to determine a number of fundamental physical processes to refine the design to be robust enough to operate with the wide variety of crude oils, weathering processes, and emulsions that can occur in the course of an oil spill. Primarily, we need to determine how the evaporation and combustion timescales for emulsified droplets relate to the oil properties, dispersant properties, seawater fraction, and imposed heat transfer and temperature surrounding the droplet. We can use these data to determine the necessary residence time at the base of the plume for stable combustion and the necessary residence time along the length of the plume for complete combustion for the wide variety of crude oils and mixtures that need disposal.

ACKNOWLEDGEMENT

This study was funded in part by the U. S. Department of the Interior, Bureau of Safety and Environmental Enforcement (BSEE), through Inter-agency Agreement No. E12PG00050 with the Naval Research Laboratory (NRL), as part of the BSEE Oil Spill Response Research Program.

This final report has been reviewed by the BSEE and approved for publication. Approval does not signify that the contents necessarily reflect the views and policies of the BSEE, nor does mention of the trade names or commercial products constitute endorsement or recommendation for use.

PERSONNEL

The Navy Technology Center for Safety and Survivability of the Naval Research Laboratory has an established history of successfully supporting the combustion and fire testing of the Navy's facilities and operations.

Dr. Steven Tuttle is a Research Mechanical Engineer and Acting Head of the Combustion Dynamics and Modeling Section in the Navy Technology Center for Safety and Survivability (NTCSS) at the U.S. Naval Research Laboratory. Dr. Tuttle worked in the gas turbine industry for over six years while managing and conducting his doctoral research at the University of Connecticut. As an engineer, he developed and validated heat transfer, thermoacoustic, and spray combustion stability models for technology development and demonstration. At the same time, he directed and managed funding to the University of Connecticut that supported his doctoral research and that of others. As a student, he designed and built an afterburner combustion experiment and the associated electronic fuel control and safety system. Dr. Tuttle mentored undergraduates and led the team of MS and PhD students as they conducted experiments and measured the fuel, flowfield, and combustion behavior. For his postdoctoral studies, he was the principle investigator for velocity measurements of a reacting scramjet cavity and shear layer at the U.S. Air Force Research Laboratory. He joined the staff at NRL in 2011, where he is the principle investigator studying spray combustion of alternative fuels and collaborates with other NRL investigators in projects ranging from fuel sensing to fire characterization.

Mr. John P. Farley is Director Chesapeake Bay Detachment/ ex-USShadwell Fire Test Operations, NTCSS. He earned his B.S. degree from Lowell Technological Institute in mathematics in 1974 and his M.A. degree from the University of Rhode Island in marine affairs in 1981. Prior to joining NRL, he served as a surface line officer, which included shipboard assignments on the USS Vesole (DD-878), USS Okinawa (LPH-3), USS Jesse L. Brown (FF-1089), USS Josephus Daniels (CG-27), and the USS Connole (FF-1056). He joined the Navy Technology Center for Safety and Survivability of the Naval Research Laboratory's Chemistry Division in 1994, where he has worked as the Project Officer for the Navy's fire test ship ex-USS Shadwell developing new fire protection technologies and firefighting

doctrine for the naval surface and submarine forces. While assigned to NRL, he has been awarded the Legion of Merit for exceptional meritorious service in 1997, two Alan Berman Research Publication awards for 1997 and 2004, and the 2003 RINA – Lloyd's Register Safer Ship Award.

Dr. James W. Fleming is a research chemist and former Head of the Combustion Dynamics and Modeling Section of the NTCSS at the Naval Research Laboratory, Washington, DC. Dr. Fleming's research interests are in flow dynamics and reactive systems. He has investigated the fundamental reaction kinetics of important flame radicals, nitrogen combustion chemistry relevant to atmospheric pollution and energetic materials, the behavior of high-pressure solid propellant flames, combustion chemistry in low pressure and atmospheric pressure flames, and flame suppression chemistry including the suppression properties of aerosols and aqueous foams. He is a member of the American Chemical Society, the American Physical Society, the Combustion Institute, and former member of the Editorial Board of Combustion and Flame.

REFERENCES

[1] Buist, I. A., "Disposal of Spilled Hibernia Crude Oils and Emulsions: In-Situ Burning and the "Swirlfire" Burner," *12th Arctic and Marine Oil Spill Program Technical Seminar*, Environment Canada, 1989.

[2] Tebeau, P., Murphy, M., Vicedomine, J., and Sprague, M., "Technology Assessment and Concept Evaluation for Alternative Approaches to In-Situ Burning of Oil Spills in the Marine Environment," U.S. Minerals Management Service, Herndon, Virginia, Contract No. 1435-01-97-PO14176. Marine Research Associates, LLC 158 Wyassup Road North Stonington, CT 06359.

[3] Tebeau, P. A., "Alternative Approaches to *In Situ* Burning Operations," *In Situ Burning of Oil Spills Workshop*, Building and Fire Research Laboratory, National Institute of Standards and Technology, 1998.

[4] Ocampo-Barrera, R., Villasenor, R., and Diego-Marin, A., "An experimental study of the effect of water content on combustion of heavy fuel oil/water emulsion droplets," *Combustion and Flame* Vol. 126, No. 4, 2001, pp. 1845-1855. doi: 10.1016/s0010-2180(01)00295-4

[5] LeFebvre, A. H., *Gas Turbine Combustion, 2nd Ed*, 2 ed., Taylor & Francis, Philadelphia, PA, 1999.

[6] Bennison, T., "Prediction of Heavy Oil Viscosity," *IBC Heavy Oil Field Development Conference*, IBC UK Conferences Limited, 1998.

[7] Gañán-Calvo, A. M., "Enhanced liquid atomization: From flow-focusing to flow-blurring," *Applied Physics Letters* Vol. 86, No. 21, 2005, p. 214101. doi: 10.1063/1.1931057

[8] Simmons, B. M., and Agrawal, A. K., "Spray Characteristics of a Flow-Blurring Atomizer," *Atomization and Sprays* Vol. 20, No. 9, 2010, pp. 821-835. doi: 10.1615/AtomizSpr.v20.i9.60

[9] Simmons, B. M., and Agrawal, A. K., "Flow and Dropsize Measurements in Glycerol Spray Flames," AIAA 2012-0523.

[10] Jiang, L., Kolhe, P. S., Taylor, R. P. T., and Agrawal, A. K., "Measurements in a Combustor Operated on Alternative Liquid Fuels," AIAA 2012-0524.

[11] ASTM D1141-13, "Standard Practice for the Preparation of Substitute Ocean Water", ASTM International, West Conshohocken, PA, 2013.

[12] Repas, G. A., "Hydrogen-Air Ignition Torch", NASA-TM-88882, 1986.

[13] Guy, R. W., Rogers, R. C., Puster, R. L., Rock, K. E., and Diskin, G. S., "The NASA Langley Scramjet Test Complex," American Institute of Aeronautics and Astronautics AIAA 1996-3243.

[14] Tuttle, S. G., Chaudhuri, S., Kostka Jr, S., Kopp-Vaughan, K. M., Jensen, T. R., Cetegen, B. M., and Renfro, M. W., "Time-resolved blowoff transition measurements for two-dimensional bluff body-stabilized flames in vitiated flow," *Combustion and Flame* Vol. 159, No. 1, 2012, pp. 291-305.
doi: 10.1016/j.combustflame.2011.06.001

[15] Albrecht, H. E., Borys, M., Damashke, N., and Tropea, C., *Laser Doppler and Phase Doppler Measurement Techniques*, Springer-Verlag, New York, 2003.

[16] LeFebvre, A. H., *Atomization and Sprays*, 1 ed., Hemisphere Publishing Corporation, 1989.

[17] Wang, C., Dean, A. M., Zhu, H., and Kee, R. J., "The effects of multicomponent fuel droplet evaporation on the kinetics of strained opposed-flow diffusion flames," *Combustion and Flame* Vol. 160, No. 2, 2013, pp. 265-275.
doi: 10.1016/j.combustflame.2012.10.012

[18] NFPA 58, "Liquefied Petroleum Gas Code ", National Fire Protection Association, Quincy, Massachussets, 2014.

Appendix A

CRUDE OIL ASSAY

Data Comparison of Selected Crude Oils

COUNTRY	Ecuador
STATE	
CRUDE	Oriente Heavy Exp Bld (CVX) '10
REFERENCE	ORINT234-L
SAMPLE DATE	2010
ANALYSIS QUALITY	A
WHOLE CRUDE INSPECTIONS	
Gravity, °API	23.4
Specific Gravity	0.9135
Sulfur, wt %	1.48
Mercaptan Sulfur, ppm	2.00
Dissolved H2S, ppm	0.000268
Nitrogen, ppm	2980
Pour Point °F	-21.2
Pour Point °C	-29.6
Acid Number, mg KOH/g	0.100
Back-Blended Acid, mg KOH/g	0.0402
Viscosity @ 40 °C (104 °F), cSt	48.1
Viscosity @ 50 °C (122 °F), cSt	31.3
Asphaltenes, C7, %	8.91
Nickel, ppm	70.8
Vanadium, ppm	175
Characterization Factor, K	11.77
MCR, wt%	9.86
TBP YIELDS, VOL %	
Butanes and Lighter	0.918
Light Gasoline (55-175 °F)	2.832
Light Naphtha (175-300 °F)	8.297
Heavy Naphtha (300-400 °F)	7.267
Kerosene (400-500 °F)	8.244
Atm. Gas Oil (500-650 °F)	14.304
Lt Vacuum Gas Oil (650-800 °F)	13.627
Hvy Vacuum Gas Oil (800-1050 °F)	19.186
Vacuum Residuum (1050 °F+)	25.326

LIGHT GASOLINE (55-175 °F)

Gravity, °API	81.5
Specific Gravity	0.6643
Mercaptan Sulfur, ppm	0.289
Octane Number, Research, Clear	74.4

LIGHT NAPHTHA (175-300 °F)

Gravity, °API	56.4
Specific Gravity	0.7531
Mercaptan Sulfur, ppm	1.13
Naphthenes, vol %	44.15
Aromatics, vol %	8.28
Octane Number, Research, Clear	61.5

HEAVY NAPHTHA (300-400 °F)

Gravity, °API	46.3
Specific Gravity	0.7959
Sulfur, wt %	0.0378
Mercaptan Sulfur, ppm	1.42
Naphthenes, vol %	49.46
Aromatics, vol %	11.58
Smoke Point, mm (ASTM)	24.7

KEROSENE (400-500 °F)

Gravity, °API	38.3
Specific Gravity	0.8335
Sulfur, wt %	0.321
Mercaptan Sulfur, ppm	2.26
Naphthenes, vol %	50.72
Aromatics, vol %	16.82
Freezing Point, °F	-49.7
Freezing Point, °C	-45.4
Smoke Point, mm (ASTM)	19.2
Acid Number, mg KOH/g	0.0188
Viscosity @ 50 °C (122 °F), cSt	1.54

ATM. GAS OIL (500-650 °F)

Gravity, °API	32.0
Specific Gravity	0.8655
Sulfur, wt %	0.915
Nitrogen, ppm	97.0
Acid Number, mg KOH/g	0.0304
Pour Point °F	4.8
Pour Point °C	-15.1
Viscosity @ 50 °C (122 °F), cSt	3.59
Cetane Index	51.2
Characterization Factor, K	11.70

ATM. RESIDUUM (650 °F+)

Yield, vol%	58.139
Gravity, °API	11.8
Specific Gravity	0.9874
Sulfur, wt %	2.10
Nitrogen, ppm	4700
MCR, wt%	15.6
Asphaltenes, C7, %	14.1
Nickel, ppm	112
Vanadium, ppm	278
Pour Point °F	83.4
Pour Point °C	28.6
Viscosity @ 50 °C (122 °F), cSt	4140
Viscosity @ 100 °C (212 °F), cSt	215
Characterization Factor, K	11.64

LT VAC. GAS OIL (650-800 °F)

Gravity, °API	24.2
Specific Gravity	0.9087
Sulfur, wt %	1.40
Nitrogen, ppm	822
Naphthenes, vol %	46.48
Paraffins, vol%	19.32
Pour Point °F	56.9
Pour Point °C	13.8
Acid Number, mg KOH/g	0.0469
Aniline Point, °F	166.9
Aniline Point, °C	75.0
Hydrogen, wt%	12.61
Viscosity @ 50 °C (122 °F), cSt	14.5
Viscosity @ 100 °C (212 °F), cSt	3.84
Characterization Factor, K	11.65

HVY VAC. GAS OIL (800-1050 °F)

Gravity, °API	19.1
Specific Gravity	0.9399
Sulfur, wt %	1.67
Nitrogen, ppm	2220
MCR, wt%	1.26
Nickel, ppm	1.62
Vanadium, ppm	4.33
Pour Point °F	106.1
Pour Point °C	41.1
Acid Number, mg KOH/g	0.0640
Aniline Point, °F	185.1
Aniline Point, °C	85.1
Hydrogen, wt%	12.09
Viscosity @ 50 °C (122 °F), cSt	174
Viscosity @ 100 °C (212 °F), cSt	18.6
Characterization Factor, K	11.84

VACUUM RESIDUUM (1050 °F+)

Yield, vol%	25.326
Gravity, °API	1.3
Specific Gravity	1.0658
Sulfur, wt %	2.71
Nitrogen, ppm	8140
Hydrogen, wt%	10.02
MCR, wt%	32.4
Asphaltenes, C7, %	30.0
Nickel, ppm	238
Vanadium, ppm	588
Pour Point °F	277.0
Pour Point °C	136.1
Viscosity @ 50 °C (122 °F), cSt	48400000000
Viscosity @ 100 °C (212 °F), cSt	5300000
Viscosity @ 135 °C (275 °F), cSt	109000
Cutter, vol% in Fuel Oil	46.9
Fuel Oil Yield, vol%	47.7
Characterization Factor, K	11.6